

SELF-SEEDING DESIGN FOR SwissFEL

E. Prat and S. Reiche, PSI, Villigen, Switzerland

Abstract

The SwissFEL facility, presently under construction at the Paul Scherrer Institute, will provide SASE and self-seeded FEL radiation at a hard (1-7 Å) and soft (7-70 Å) X-ray FEL beamlines. This paper presents the current status of the self-seeding design for SwissFEL. The layout and full 6D start-to-end simulation results are presented for the hard X-ray beamline. Studies for different charges and optimization of the first and second undulator stages are shown.

INTRODUCTION

Seeding for FELs has several advantages in comparison to SASE radiation: the longitudinal coherence is increased and therefore the FEL brilliance is improved, the pulse to pulse central wavelength is stabilized, the temporal pulse shape is smoothed, the gain length is reduced, etc.

Up to now self-seeding is the only seeding strategy that has been demonstrated with a hard X-ray FEL [1, 2]. A proof-of-principle experiment of the self-seeding scheme based on the proposal of Geloni et al [2] was successfully carried out at LCLS for hard X-rays at the beginning of 2012 [3]. For soft X-rays, self-seeding [4] is presently the only seeding scheme that does not exhibit stringent short wavelength limitations, like all laser-based approaches do, therefore being the most robust and lowest risk strategy to seed a soft X-ray [5]. Self-seeding operation is planned at SwissFEL at 2017 for the hard X-ray beamline for a wavelength down to 1 Å, and at a later phase for the soft X-ray beamline down to a wavelength of 1 nm [6].

Figure 1 shows a generic layout of the self-seeding scheme for soft and hard X-rays. The first undulator stage produces standard SASE-FEL radiation. After that the FEL radiation goes through a monochromator, while the electron beam travels through a magnetic chicane. In the second undulator stage the transmitted radiation overlaps with the electron beam to produce seeded-FEL radiation. The magnetic chicane has three functions: it delays the electron to allow the longitudinal overlap between the electron and photon beams, it smears out the electron bunching created at the first undulator section, and it separates the electrons from the radiation so that intercepting optical elements for the filtering of the X-rays can be placed. The first undulator stage works in the exponential regime before saturation to avoid a blow-up of the energy spread of the electron beam that would prevent the beam to amplify the FEL signal in the second stage. At the same time it has to provide sufficient FEL radiation so that the seed power is well above the shot-noise level at the second undulator stage. The difference between the hard and the soft X-ray is the method to produce a monochromatized signal: for soft X-rays a grating monochromator can be used, while for hard X-rays a Bragg-crystal (e.g. diamond) is employed. For both

cases the intersection with the monochromator and the chicane can be presently placed in a space of about 4 m length, i.e. the space occupied by a SwissFEL undulator module.

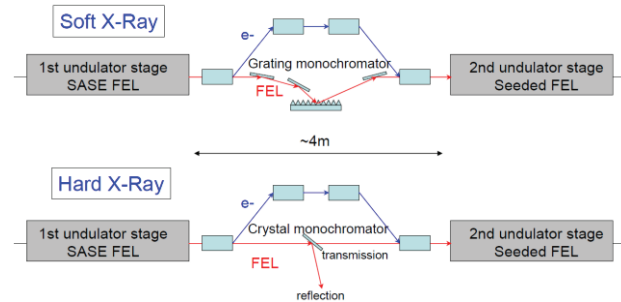


Figure 1: Generic layout of the self-seeding scheme.

SwissFEL will operate with electron beam charges varying between 10 and 200 pC. A study for the hard X-ray beamline for 10 pC using design parameters was shown one year ago at this conference [7]. The main goal of the present work is to analyze if it is possible to produce saturated self-seeded FEL at 200 pC within the available space and equipment (12 undulator modules and the chicane). This time we have used electron distributions obtained from start-to-end calculations as an input for the FEL simulations. We have also redone the simulations for 10 pC with the start-to-end simulation distribution of the electron beam. For both charges we have optimized the number of modules to be used at the first stage (thus the location of the monochromator chicane) and we have applied detuning and tapering to maximize the FEL performance at the second stage. Concerning the soft X-ray beamline, a design based on nominal beam parameters for 200 pC was already done [7]. However, it is still pending to confirm this design with parameters obtained from start-to-end calculations.

LAYOUT AND SIMULATIONS SETUP

The present design lattice for the hard X-ray beamline consists of 12 undulator modules. Each of them is 4 m long, has a period length of 15 mm and a variable gap. The distance between modules is 0.75 m. In addition we have reserved the same space for the crystal monochromator and the chicane. The facility is able to accommodate up to seven more modules for potential future upgrades such as tapering. The beam energy is between 2.1 GeV and 5.8 GeV, corresponding to a radiation wavelength range between 1 Å and 7 Å. The present study is done for a wavelength of 1 Å.

The four dipoles of the magnetic chicane are 0.4 m long each and can deflect the electron beam up to an angle of half a degree at 6 GeV. The drifts between the first and second dipole and between the third and fourth magnet are about 0.35 m long, and the distance between the

second and third dipole is about 1.4 m. This is sufficient to provide a time delay to the electron beam of more than 100 fs.

The FEL interaction is simulated with *Genesis* [8]. For the monochromator we use a model based on dynamic diffraction theory, which agrees with the model developed by Gelsoni et al [2] that reconstructs the transmission function of the Bragg-crystal based on the Kramers-Kronig relation.

Figure 2 shows the properties of the electron beam distribution for 200 pC and 10 pC that we used as input for the FEL simulations. The distributions have been obtained by tracking with the simulation codes *ASTRA* [9] and *elegant* [10]. The goal is to obtain the same FEL performance for all charges, so the peak current is adjusted to compensate the different emittance values for different charges – the quantity $I \cdot (\epsilon_x \epsilon_y)^{-1/2}$ is kept constant to yield the same gain length. We have chosen the average β -function along the undulator that minimizes the FEL gain length. The optimum value is around 10 m for both electron beam charges.

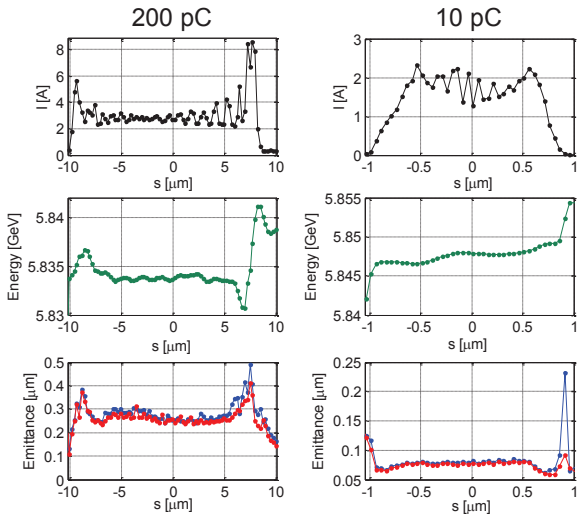


Figure 2: Electron beam properties at the undulator entrance obtained from start-to-end simulations.

SIMULATION RESULTS FOR 200 pC

We have optimized the number of modules to be placed in the first undulator stage. The number of modules was varied between two and six. For each setting we placed a total of 12 undulator modules for the whole beamline. For each case, five simulations were carried out with different shot noise seeds. The undulator field in the second stage was reduced to compensate the energy loss of the electron beam in the first stage.

Figure 3 shows the seed generated in the monochromator for the case with four modules in the first stage. The optimum delay in the second stage to overlap the electron beam with the crystal wake is about 75 fs. The bunch length is sufficiently long to resolve the two individual frequencies of the beat wave.

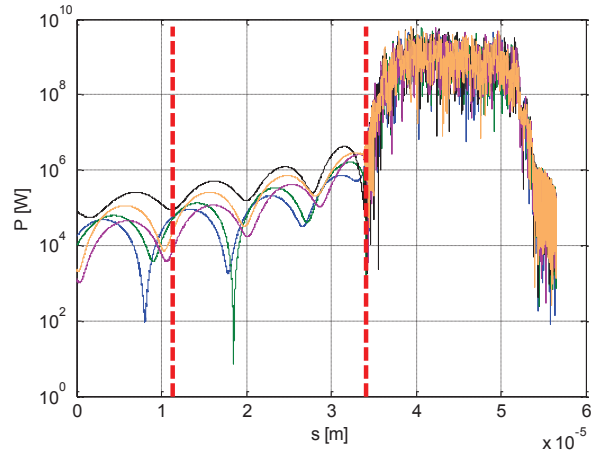


Figure 3: SASE FEL of the first stage and wake generated in the crystal (logarithmic scale) when four modules are used in the first stage. Every plotted line corresponds to a different seed. The part between the red dashed lines is seeded in the second stage.

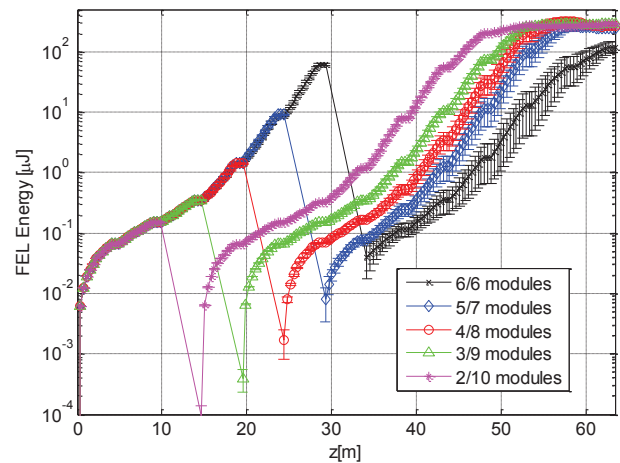


Figure 4: FEL macropulse energy for different number of modules in stage 1 for 200 pC (logarithmic scale). The plotted errors are the statistical variations of the five runs.

Figure 4 shows the FEL power along the undulator beamline for the different considered cases. The first conclusion is that it is possible to achieve saturation within 12 undulator modules. Table 1 indicates the FEL macropulse energy, the number of required modules to reach saturation, and the bandwidth at the end of the second undulator stage for the different cases. We choose the solution with four modules in the first stage since it gives excellent FEL performance and only 11 modules are required to reach saturation, and therefore one module can be foreseen as a reserve. By using five modules in the first stage the spectrum bandwidth would be even smaller, but all 12 modules would be needed to reach saturation. The solution with three modules in the first stage is not satisfactory since there is a significant SASE contribution to the FEL in the second stage. For two modules in the first stage this SASE contribution is even bigger and

comparable to the seed power, and therefore the spectrum bandwidth is much larger. Finally, for six modules in the first stage saturation can not be reached with 12 modules, since the energy spread at the exit of the first stage is too high by near saturation blow-up in the first stage.

Table 1: Seeded FEL performance (200 pC case). The errors are the statistical variations of the five runs.

Modules configuration	Energy [μJ]	Modules to saturation	Spectrum bandwidth (FWHM)
6/6	83 ± 18	> 12	$1.48\text{e-}5 \pm 0.70\text{e-}5$
5/7	250 ± 9	12	$1.33\text{e-}5 \pm 0.33\text{e-}5$
4/8	256 ± 11	11	$2.34\text{e-}5 \pm 0.58\text{e-}5$
3/9	296 ± 7	10	$2.02\text{e-}5 \pm 1.44\text{e-}5$
2/10	296 ± 3	9	$7.48\text{e-}4 \pm 4.19\text{e-}4$

All the simulations presented below are considering four modules in the first stage and eight in the second one. Figure 5 shows the spectrum after the first undulator stage (SASE) and after the second section (seeded radiation) for the five simulations with different shot-noise seeds. The bandwidth is reduced by a factor of 40.

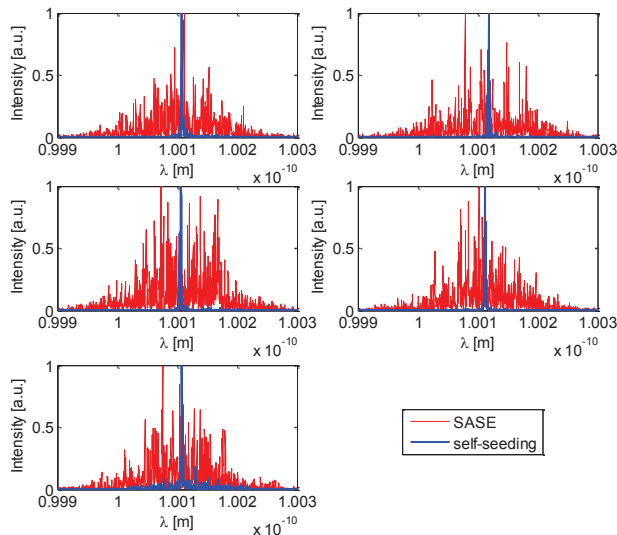


Figure 5: Spectrum for self-seeding (blue) and SASE (red) in the 4/8 modules configuration (200 pC case).

The performance of the second FEL stage can be optimized by detuning and tapering. Apart from compensating for the energy loss in the first stage, detuning the undulator field also allows the electrons to resonate with the FEL radiation longer than for the resonant case [11]. We have chosen the undulator field that minimizes the gain length in the second stage. The optimum detuning was found to be with the undulator parameter reduced by 0.14 % with respect to the value in the first stage.

In addition to the detuning we have introduced linear tapering in the last three modules to maximize the FEL

energy: we have regularly decreased the field strength to allow the electrons with lower energy to maintain the resonance condition with the FEL radiation, therefore increasing the FEL power beyond the saturation level. We have done the simulations for one representative case of the five shot noise realizations. The maximum FEL energy corresponds to a linear taper amplitude of 0.4%. The final FEL energy increases from about 0.26 mJ to 0.65 mJ. Figure 6 shows the FEL power along the whole undulator beamline for the chosen configuration, with and without optimization.

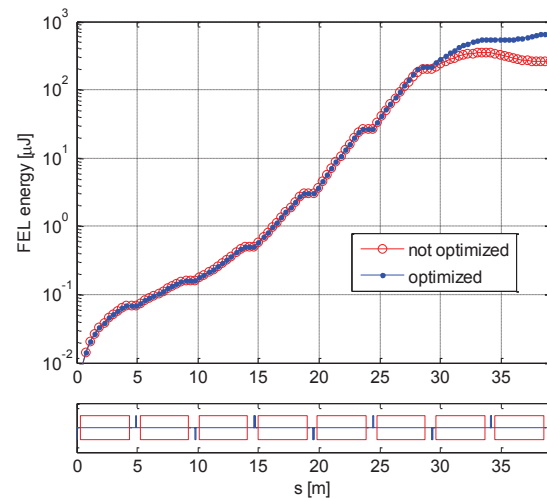


Figure 6: Radiation power with and without optimization for the 200 pC case (logarithmic scale).

SIMULATION RESULTS FOR 10 pC

We have done the same study for 10 pC: we have performed simulations for different number of modules in the first stage and optimized the second stage by detuning and tapering. We have run five simulations per each configuration. For the 10 pC case, the optimum delay to overlap the electrons with the seed is about 15 fs.

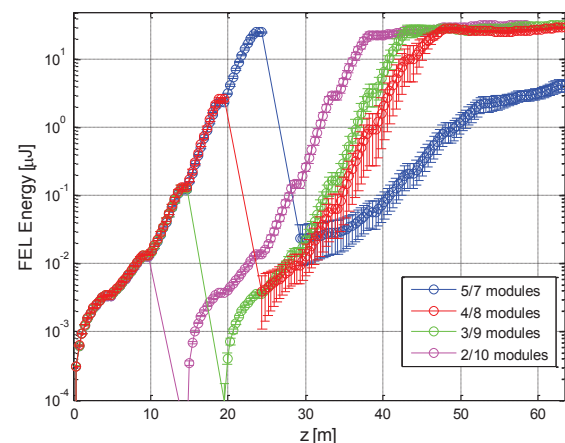


Figure 7: FEL macropulse energy for different number of modules in stage 1 for the 10 pC case (logarithmic scale).

Figure 7 and Table 2 show the results for the different cases considered. The optimum number of modules in the first stage is four, as in the 200 pC case, since it gives the smallest spectrum bandwidth. For three or two modules in the first stage the SASE contribution in the second stage is too high, which results in a larger spectral bandwidth. With five modules the FEL almost reaches saturation in the first stage, resulting in a too high energy spread which significantly limits the power in the second stage.

Table 2: Seeded FEL performance (10 pC case). The errors are the statistical variations of the five runs.

Modules configuration	Energy [μJ]	Modules to saturation	Spectrum bandwidth (FWHM)
5/7	4.2 ± 0.9	>12	1.06e-3 ± 0.93e-3
4/8	29.8 ± 0.3	8	6.70e-5 ± 0.29e-5
3/9	32.6 ± 0.9	8	2.05e-4 ± 1.40 e-4
2/10	32.7 ± 1.3	7	5.19e-4 ± 6.86 e-4

All the simulations presented below are considering the optimum configuration of 4/8 modules. Figure 8 shows the spectrum after the first and second undulator stages. The bandwidth gets reduced by a factor of 10.

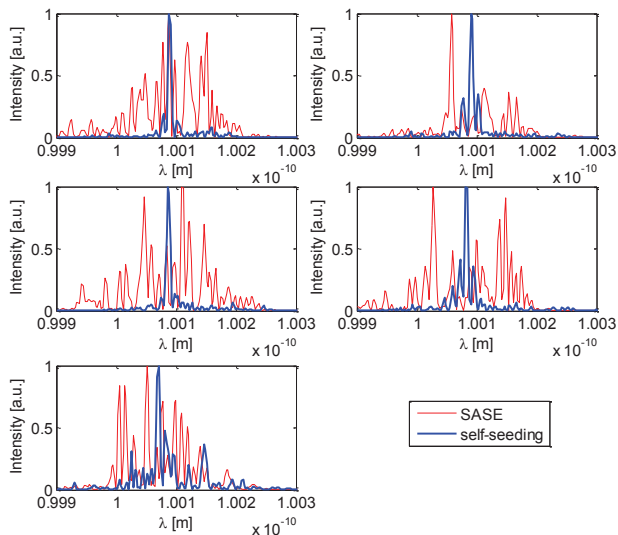


Figure 8: Spectrum for self-seeding (blue) and SASE (red) in the 4/8 modules configuration (10 pC case).

The second undulator stage has been optimized by detuning and tapering for the case with four modules in the first stage. One of the five shot noise realizations was chosen as a representative case for this. The resonant wavelength of the second undulator stage was varied by detuning the undulator parameter in order to minimize the gain length. The optimum detuning was found to be with the undulator parameter reduced by 0.14% – for this value the gain length gets reduced by about 15%. We have also applied linear tapering in the last four modules to maximize the FEL energy. The optimum corresponds to a taper amplitude of 1.0 %. The final FEL energy improves

from 29 μJ to 81 μJ. Figure 9 shows the FEL performance at the second undulator section for the representative case, with and without optimization.

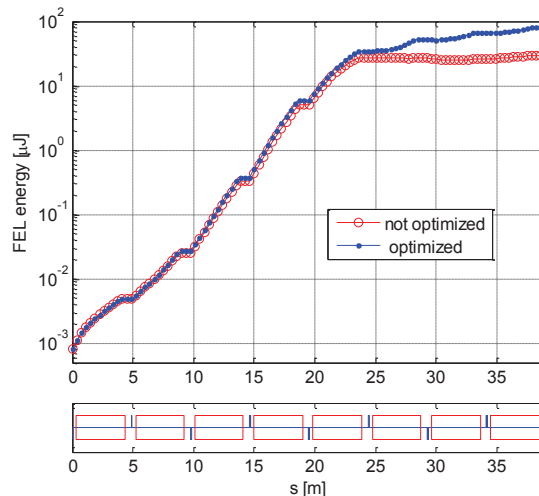


Figure 9: Radiation power with and without optimization for the 10 pC case (logarithmic scale).

CONCLUSIONS AND OUTLOOK

The presented results for the hard X-ray beamline of SwissFEL indicate that it is possible to generate saturated self-seeded FEL pulses within the present available space (12 modules and the chicane). The optimum configuration – for both 200 and 10 pC cases – is with 4 modules in the first stage and 8 modules in the second one.

Full 6D start-to-end simulations will be performed for the soft X-ray beamline of SwissFEL. A “dechirper” [12] will be used to remove the residual energy chirp of the beam coming from the linac section. Further work on the design of the monochromators for the two beamlines will be done. For the hard X-ray beamline we will also study how to further optimize the second undulator stage through tapering if more undulator modules become available in a future upgrade.

ACKNOWLEDGMENTS

We thank Simona Bettoni and Bolko Beutner for the work to generate the particle distributions that we used as input for the FEL simulations.

REFERENCES

- [1] E. Saldin et al, NIM A 475 357 (2001).
- [2] G. Geloni et al, DESY report 10-053 (2010).
- [3] P. Emma et al, Nature Photonics 6, 693-698 (2012).
- [4] J. Feldhaus et al, Opt. Commun. 140, p.341 (1997).
- [5] J. Corlett et al, Final Report of “Realizing the Potential of Seeded FELs in the Soft X-Ray Regime”, Berkeley, United States, October 2011.
- [6] R. Ganter et al, PSI-Bericht 10-04.
- [7] E. Prat and S. Reiche, Proceedings of the FEL 12, Nara, Japan, 281-284 (2012).

- [8] S. Reiche, "GENESIS 1.3 User Manual", 2004.
- [9] K. Floettmann, ASTRA - A Space Charge Tracking Algorithm. DESY, Hamburg, Germany.
- [10] M. Borland, "elegant: A Flexible SDDS-Compliant Code for Accelerator Simulation", Advanced Photon Source LS-287, September 2000.
- [11] X. J. Wang et al, Appl. Phys. Lett. 91, 181115 (2007).
- [12] K. L. F. Bane and G. Stupakov, SLAC-PUB-14925 (2012)